Supplementary Information:

Act1 mediates IL-17-induced EAE pathogenesis selectively in NG2$^+$ glial cells

Zizhen Kang,[1,2] Chenhui Wang,[2] Jarod Zepp,[2] Ling Wu,[2] Kevin Sun[2], Junjie Zhao[2],Unni Chandrasekharan,[3] Paul E. DiCorleto,[3]Bruce D. Trapp,[4] Richard M. Ransohoff,[4,5,6] Xiaoxia Li[2,*]

[1]Shanghai Institute of Immunology, Shanghai Jiao Tong University School of Medicine, Shanghai, China.
[2]Department of Immunology
[3]Department of Cellular and Molecular Medicine
[4]Department of Neuroscience
[5]Neuroinflammation Research Center
[6]Mellen Center for MS Treatment and Research
Cleveland Clinic, Cleveland, OH, USA

*Correspondence should be addressed to Xiaoxia Li, lix@ccf.org

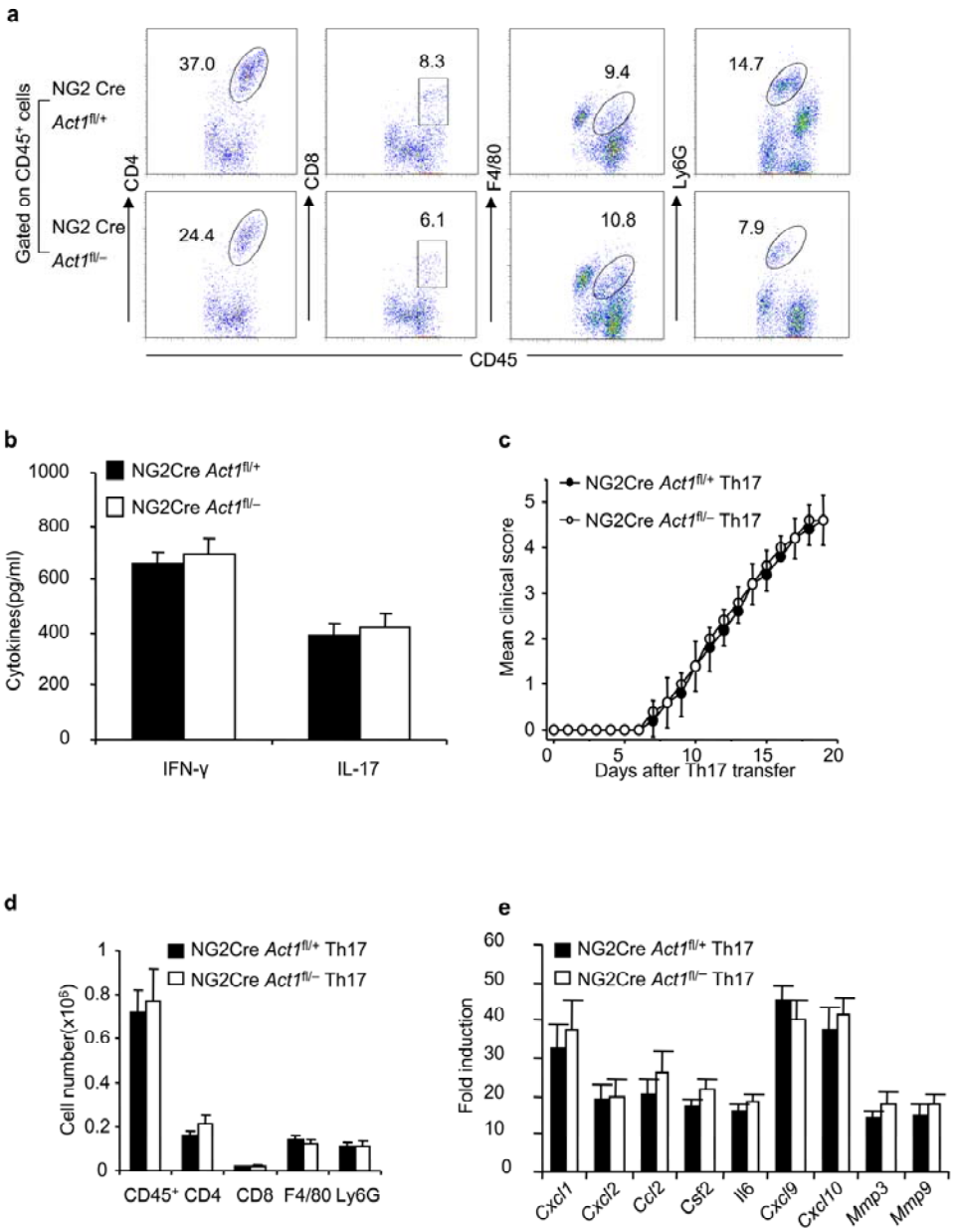

Supplementary Figure 1 Th17 cells from NG2Cre Act1$^{fl/–}$ mice can induce EAE. (a) Flow cytometric analysis show the frequency of different subsets of infiltrated leucocytes in brains of NG2Cre *Act1*$^{fl/+}$ and NG2Cre*Act1*$^{fl/–}$ mice 20 days after Th17 cell transfer. (b)Draining lymph node cells from NG2Cre*Act1*$^{fl/+}$ and NG2Cre*Act1*$^{fl/–}$ mice 10 days after immunization with MOG_{35-55} were re-stimulated with MOG_{35-55} in vitro for 4 days, followed by ELISA assay of IL-17 and IFN-γ. (c) Mean clinical score of EAE in wild-type recipient mice induced by MOG_{35-55}-specific NG2Cre*Act1*$^{fl/–}$ Th17 or NG2Cre*Act1*$^{fl/+}$ Th17 cells. (d) Absolute number of immune cell infiltration in the brains of EAE mice as indicated (19 days after Th17 transfer). (e) Real-time PCR analysis of inflammatory gene expression in the spinal cords of EAE mice as indicated. Data are representative of three independent experiments. n=5/group in each experiment. Error bars, SEM. p>0.05 at b-d.

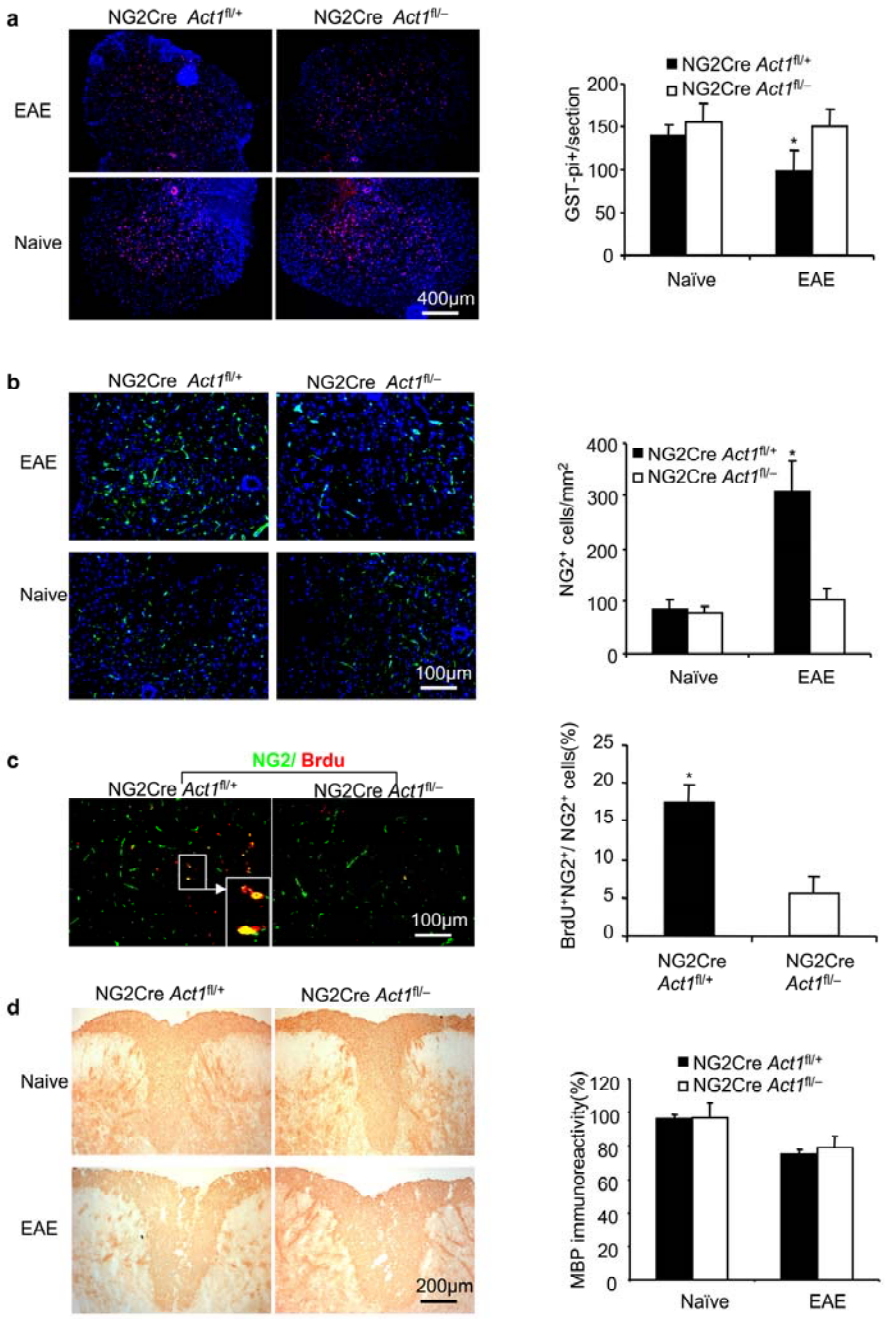

Supplementary Figure 2 Change of oligodendroglia in the NG2Cre*Act1*$^{fl/+}$ and NG2Cre*Act1*$^{fl/–}$ mice before and after EAE. NG2Cre*Act1*$^{fl/+}$ and NG2Cre*Act1*$^{fl/–}$ mice subjected to EAE by Th17 adoptive transfer(a-c) or Th1 adoptive transfer(d). (a) GST-pi^{+} cells per section were counted from lumber spinal cords of NG2Cre *Act1*$^{fl/+}$ and NG2Cre *Act1*$^{fl/–}$ mice before and after EAE(7 days after onset of EAE). (b) NG2^{+} cells/mm^{2} in the dorsal region were counted from lumber spinal cords of NG2Cre *Act1*$^{fl/+}$ and NG2Cre *Act1*$^{fl/–}$ mice before and after EAE(7 days after onset of EAE). (c) EAE mice were injected with BrdU at 1mg/mouse 24 hours before sacrifice, then spinal cords were collected from NG2Cre*Act1*$^{fl/–}$ and NG2Cre*Act1*$^{fl/+}$ EAE mice(7 days after onset of EAE), ratio of BrdU cells to NG2^{+} cell are shown. (d) MBP myelination in lumber spinal cords of NG2Cre*Act1*$^{fl/–}$ and NG2Cre*Act1*$^{fl/+}$ mice before and after Th1 EAE(20 days after Th1 transfer) were analyzed by immunohistochemical staining. Data are representative of three independent experiments. n=5/group in each experiment. Error bars, SEM. *p<0.05.

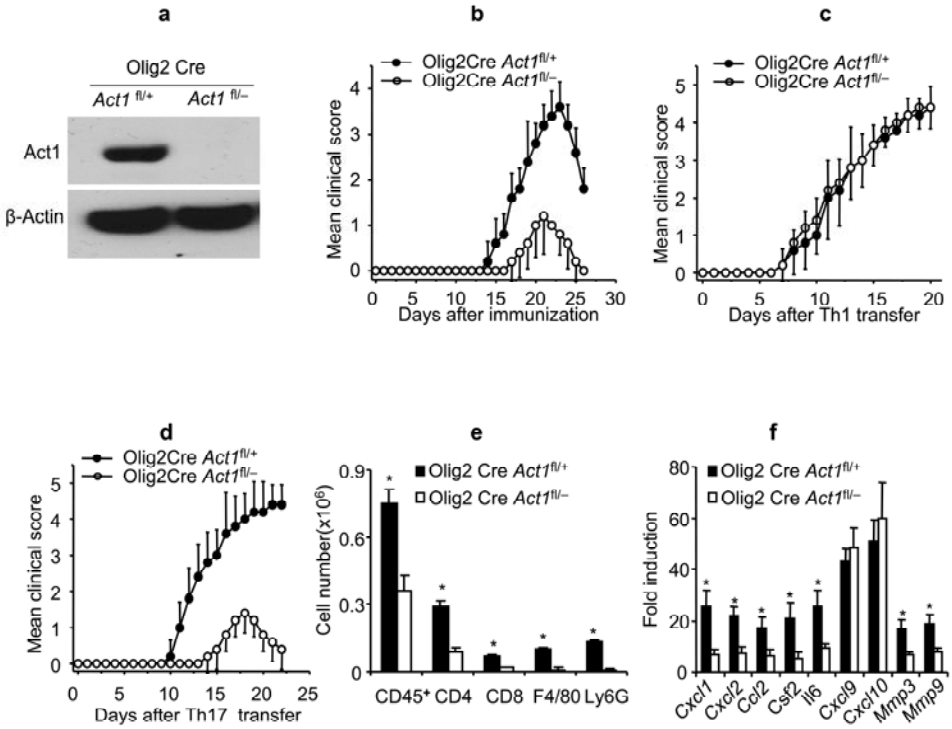

Supplementary Figure 3 Olig2 Cre-mediated ablation of Act1 in oligodendrocyte lineage ameliorates autoimmune encephalomyelitis. (a) Immunoblot analysis for the Act1 expression in cultured Olig2^{+} cells from embryonic brains. Full-length blots are presented in Supplementary Figue 5. (b) Mean clinical score of EAE in Olig2Cre*Act1*$^{fl/–}$and Olig2Cre*Act1*$^{fl/+}$ mice induced by active immunization with MOG_{35-55}($p<0.05$, two-way ANOVA). (c) Mean clinical score of EAE in Olig2Cre*Act1*$^{fl/–}$and Olig2Cre*Act1*$^{fl/+}$ mice induced by Th1 adoptive transfer ($p>0.05$, two-way ANOVA). (d) Mean clinical score of EAE in Olig2Cre*Act1*$^{fl/–}$and Olig2Cre*Act1*$^{fl/+}$ mice induced by Th17 adoptive transfer ($p<0.05$, two-way ANOVA). (e) Absolute cell numbers of infiltrated immune cells in the brains of Olig2Cre*Act1*$^{fl/–}$and Olig2Cre*Act1*$^{fl/+}$ mice (20 days after Th17 cell transfer). (f) Real-time PCR analysis of inflammatory gene expression in the spinal cords of Olig2Cre *Act1*$^{fl/–}$ and Olig2Cre*Act1*$^{fl/+}$ mice transferred with MOG_{35-55}-specific Th17 cells. Data are representative of three independent experiments. n=5/group in each experiment. Error bars, SEM; *$p<0.05$.

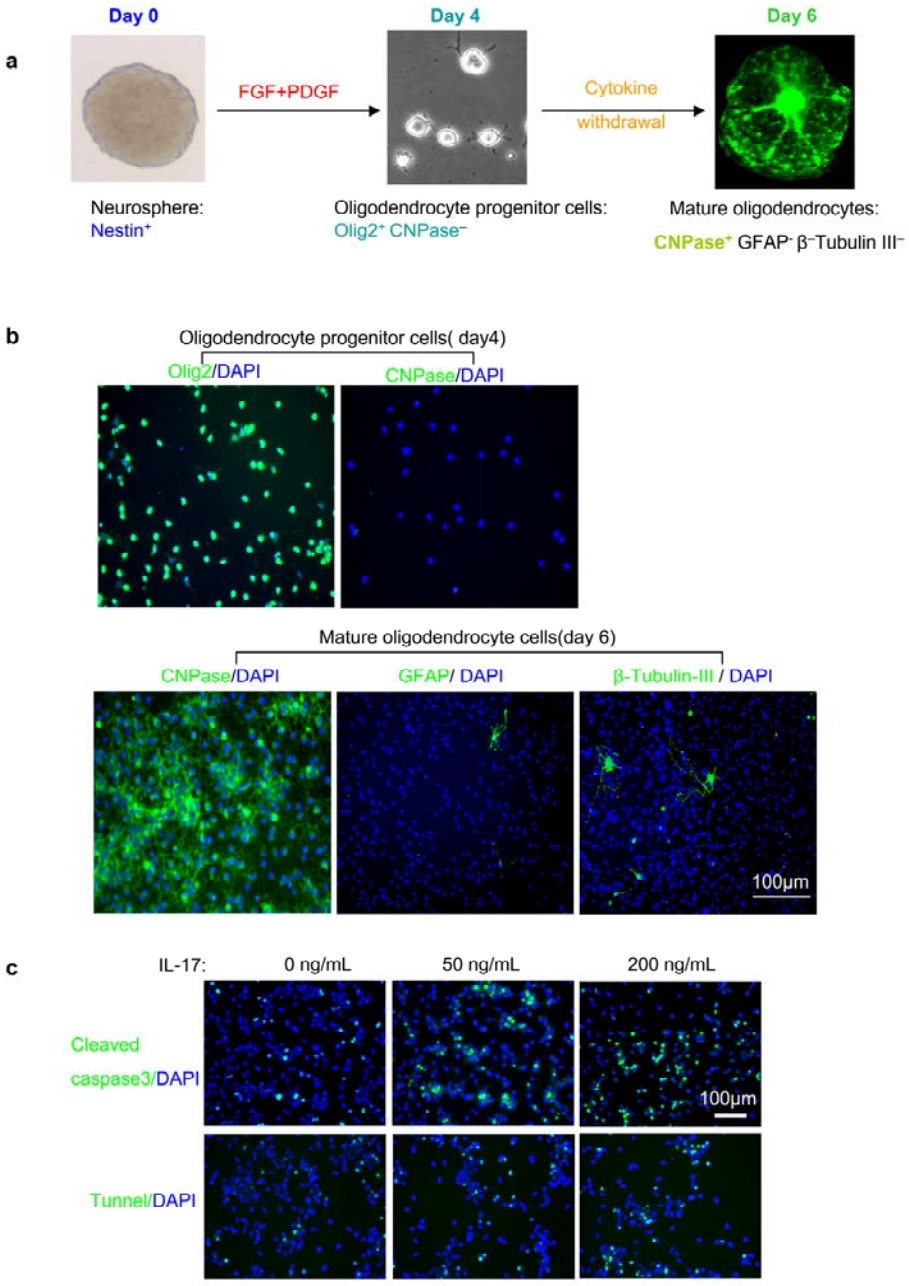

Supplementary Figure 4 Characterization of oligodendroglia cells. (a) Flow chart of oligodendroglia culture. (b) Characterization of OPCs(upper panel) and mature oligodendrocytes(lower panel). OPCs are $Olig2^{+}CNPase^{-}$ cells and mature oligodendrocytes are $CNPase^{+}$ $GFAP^{-}$ β-tubulin-III^{-} cells. (c) TUNEL and cleaved caspase 3 assays indicate the apoptotic cells after a 4-day culture of wild-type OPCs with/without IL-17 as indicated. n=5 mice, Data are representative of three independent experiments.

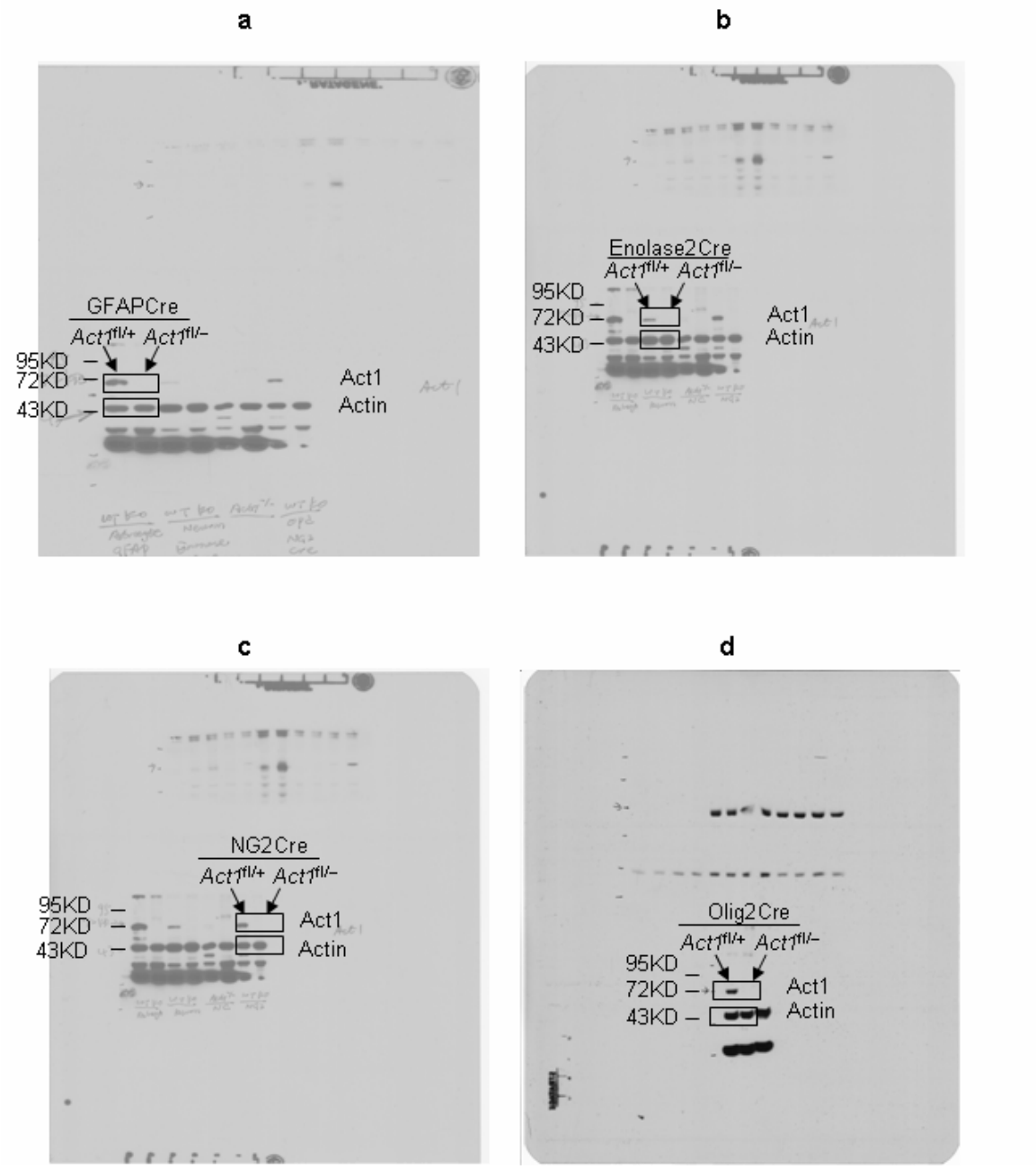

Supplementary Figure 5: Full-length immunoblots presented in Fig.1a, Fig.2a, Fig.3a and Supplemental Fig.3a. (a) Full size immunoblot for Fig.1a. (b)Full size immunoblot for Fig.2a. (c) Full size immunoblot for Fig.3a. (d) Full size immunoblot for Supplementary Fig.3a.

a

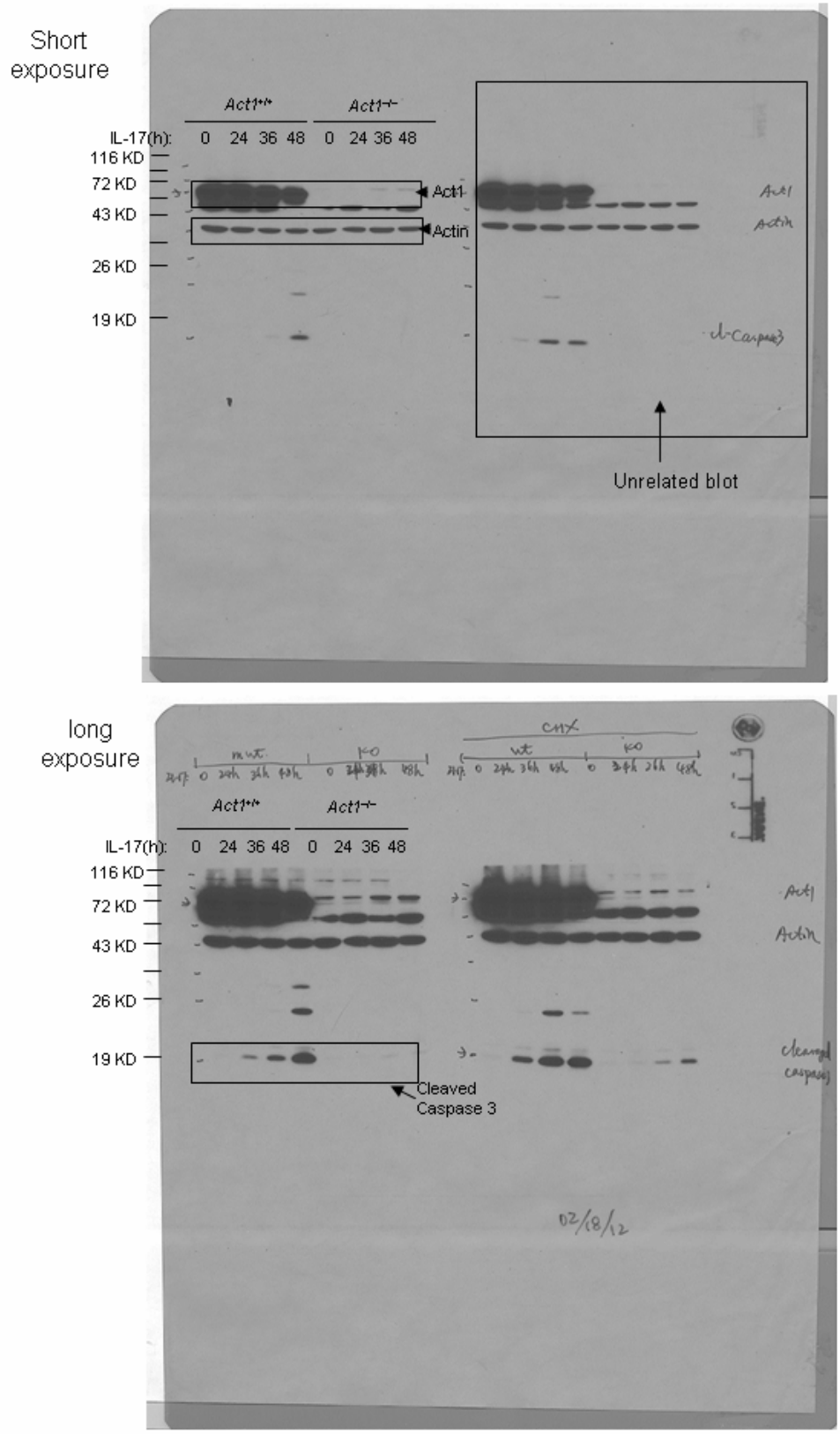

Supplementary Figure 6: Full-length immunoblots presented in Fig.6a

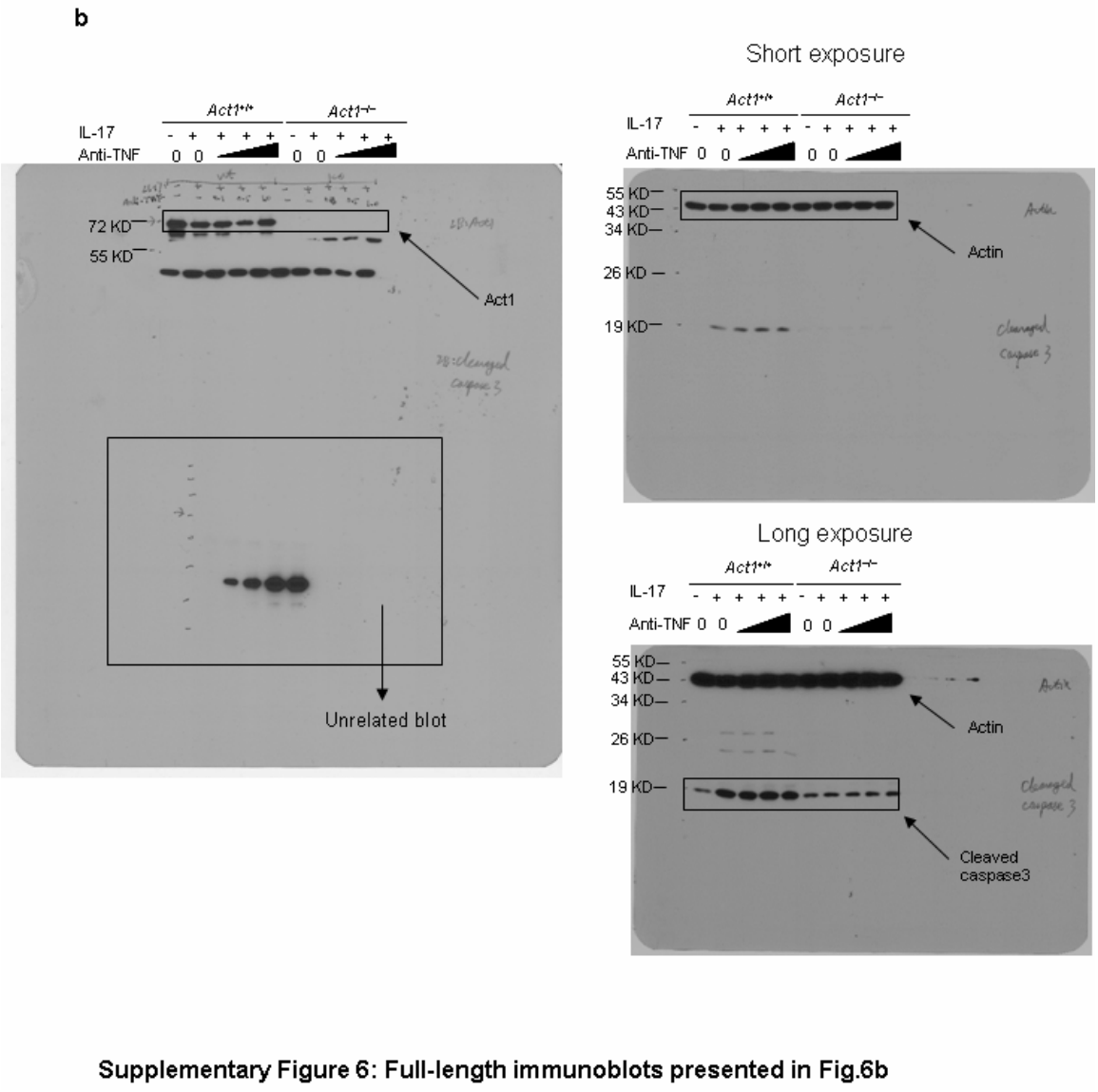

Supplementary Figure 6: Full-length immunoblots presented in Fig.6b

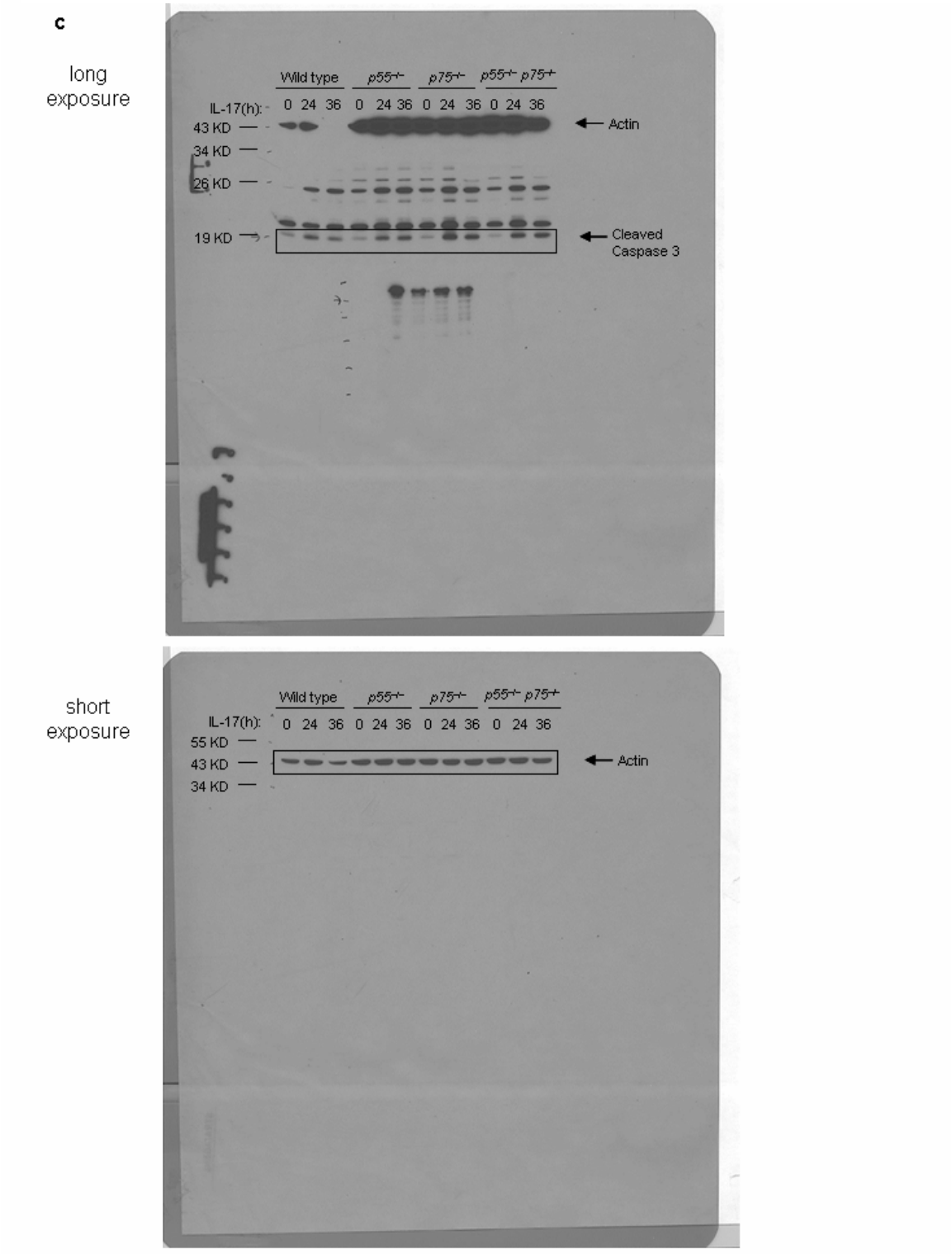

Supplementary Figure 6: Full-length immunoblots presented in Fig.6c

d

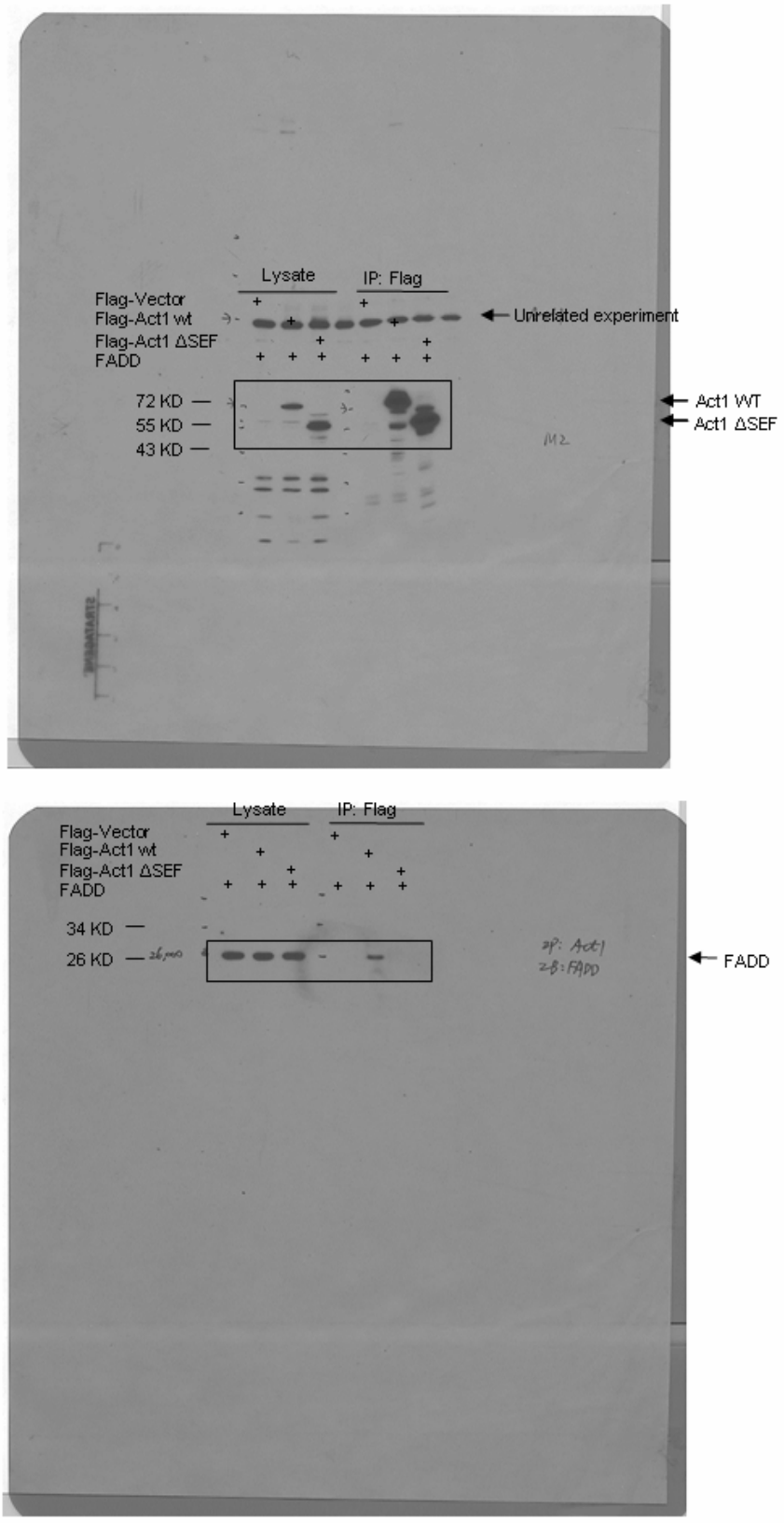

Supplementary Figure 6: Full-length immunoblots presented in Fig.6d

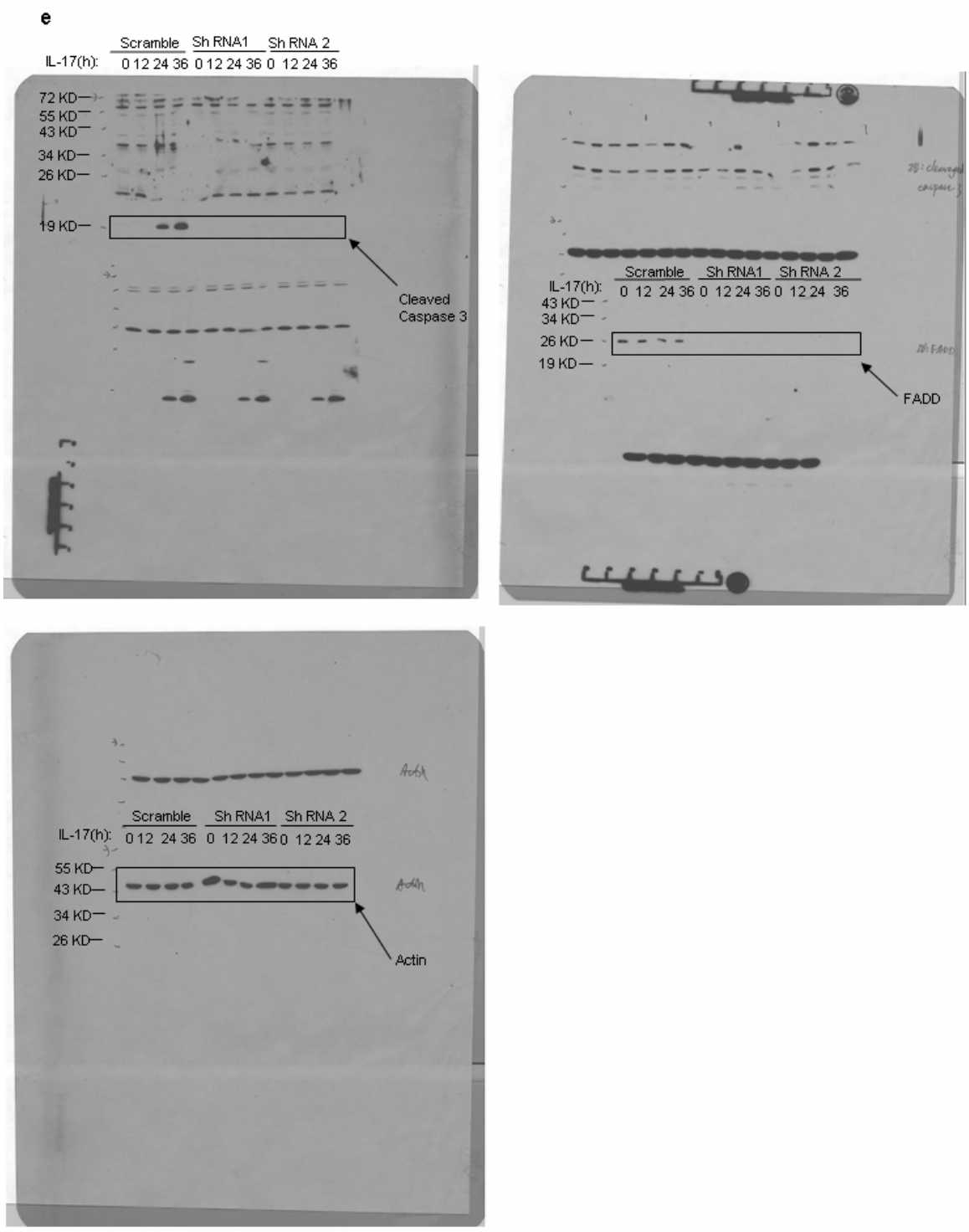

Supplementary Figure 6: Full-length immunoblots presented in Fig.6e